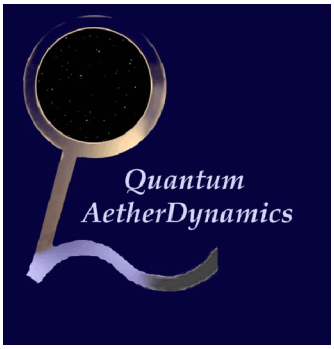

Quantum AetherDynamics Institute (QADI)

Observational Confrontation of QMU Chronogeometry: Testing Temporal-Torque Memory with Cosmic Filaments and Residual Birefringence

David W. Thomson III
Quantum AetherDynamics Institute (QADI)
Alma, Illinois, USA
ORCID: 0000-0002-5830-5427

Version 1.1 – September 18, 2026

This article is published by the Quantum AetherDynamics Institute (QADI).

It develops the Aether Physics Model (APM)

Abstract

The preceding papers of this series developed a discrete five-dimensional chronogeometric framework in which organized chronotorsional organization domains emerge naturally from the Aether Physics Model (APM) and generate observable signatures in cosmic birefringence and filamentary large-scale structure. Paper I introduced temporal-torque memory. Paper II established birefringence tomography. Paper III quantified temporal-torque observables in Quantum Measurement Units (QMU). Paper IV demonstrated numerical reconstruction methods. Paper V derived the organization of filamentary chronogeometric structures. Paper VI developed their temporal evolution equations. Paper VII produced synthetic numerical predictions.

The present work performs the first direct observational confrontation of the chronogeometric memory hypothesis.

The analysis proceeds according to

QMU Inventory → APM Mechanism → Synthetic Observable → Null Comparison → Falsifiable Prediction.

Synthetic residual birefringence maps,

$$\delta\beta(\hat{\mathbf{n}}),$$

are generated from numerical temporal-torque simulations and projected onto HEALPix skies. Angular power spectra,

$$C_\ell^{\beta\beta}, \qquad C_\ell^{E\beta}, \qquad C_\ell^{B\beta},$$

are compared against observational products and future survey forecasts. Filamentary observables are extracted from large-scale structure catalogs through measurements of filament orientation, handedness, node connectivity, and memory correlation lengths.

The objective of this work is not to assume the correctness of the Aether interpretation. Rather, it is to determine whether organized chronotorsional organization domains produce measurable observational signatures that survive direct comparison with cosmological data and remain statistically distinct from conventional models of large-scale structure formation.

Keywords: temporal torque; chronogeometric memory; cosmic birefringence; cosmic filaments; large-scale structure; observational cosmology; Aether Physics Model; Quantum Measurement Units

1 Introduction

Modern observational cosmology increasingly seeks measurable signatures that distinguish competing theories of large-scale organization. Residual cosmic birefringence, filamentary large-scale structure, and coherent orientation statistics have emerged as promising observables because they preserve information regarding the integrated evolutionary history of the Universe [Minami and Komatsu, 2020, Diego-Palazuelos et al., 2022, Sousbie, 2011, Codis et al., 2018a, Wang et al., 2021].

The preceding papers of this series [Thomson III, 2026f,a,e,d,c,b] developed a progressively constrained theoretical and computational framework describing the organization of chronotorsional organization domains within a discrete five-dimensional Aether. Paper I introduced temporal-torque memory and proposed that chronogeometric organization may persist over cosmological scales. Paper II demonstrated how residual birefringence maps may function as tomographic probes of organized temporal structure. Paper III quantified the principal observables in terms of Quantum Measurement Units (QMU). Paper IV developed numerical reconstruction methods. Paper V derived

the organization of filamentary chronogeometric structures and their predicted observables. Paper VI established temporal evolution equations governing the growth and transport of chronotorsional organization domains. Paper VII produced synthetic numerical predictions and generated simulated observational templates.

The present paper constitutes the observational capstone of that program.

Unlike the preceding papers, no new physical assumptions are introduced. The objective of this work is not to argue for the correctness of the Aether interpretation. Rather, the purpose is to determine whether the previously derived observables survive direct comparison with observational data and whether they remain statistically distinguishable from conventional cosmological models.

The scientific question considered here is intentionally narrow:

> *Can the discrete five-dimensional Aether unit produce observable memory signatures that survive direct confrontation with the sky?*

To answer this question, the paper follows a deliberately conservative methodology,

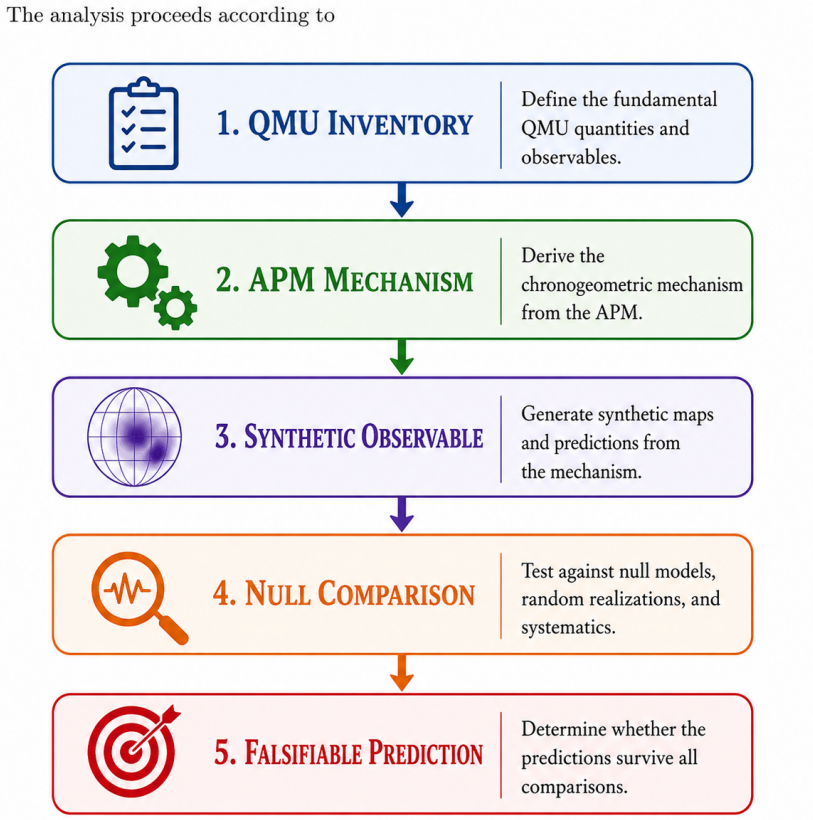

Figure 1: Overview of the analytical pipeline employed in this work.

Figure 1: The observational confrontation pipeline. The analysis proceeds from QMU inventory to APM mechanism, synthetic observable construction, null comparison, and falsifiable prediction.

The analysis proceeds according to the pipeline shown in Figure 1. Every observable considered in

this paper is derived from quantities previously established in QMU form and subjected to explicit statistical tests against null models and conventional explanations.

2 Relation to Papers I–VII

The present paper completes an eight-paper investigation into temporal-torque organization and its potential observational consequences.

Paper I introduced the concept of temporal-torque memory and proposed that organized chronogeometric domains may persist over cosmological distances [Thomson III, 2026f].

Paper II developed residual birefringence tomography and demonstrated how angular rotation fields may preserve information regarding large-scale temporal organization [Thomson III, 2026a].

Paper III introduced quantitative definitions of chronotorsional curl-organization density, chronotorsional holonomy, and associated QMU observables [Thomson III, 2026e].

Paper IV demonstrated numerical reconstruction techniques capable of generating synthetic birefringence maps from organized chronotorsional organization fields [Thomson III, 2026d].

Paper V developed the theory of filamentary chronogeometry and predicted that organized chronotorsional organization domains naturally generate coherent filamentary structures and preferred orientation statistics [Thomson III, 2026c].

Paper VI established the temporal evolution equations governing transport, organization, and persistence of chronotorsional organization domains [Thomson III, 2026b].

Paper VII implemented these equations numerically and generated synthetic observational predictions Thomson III [2026g].

The present work performs the transition

$$\text{Numerical Prediction} \rightarrow \text{Observational Confrontation}.$$

The paper therefore occupies a unique position within the series. It neither extends the theoretical framework nor introduces additional physical assumptions. Instead, it subjects the previously derived observables to direct empirical tests.

Consequently, the survival or failure of the chronogeometric interpretation depends entirely upon whether the predicted signatures remain statistically significant after confrontation with observational data and conventional models.

3 QMU Inventory and Physical Observables

The observational program developed in this paper is constructed entirely from previously defined Quantum Measurement Units and their associated chronogeometric observables [Thomson III, 2026f,a,e,d,c,b,g].

The fundamental closure relation remains Ledger One,

$$A_u \,\mathrm{curl} = {F_q}^2 {\lambda_C}^2,$$

which expresses the closure between Aether organization, temporal evolution, and propagation.

Chronogeometric organization emerges from discrete Compton-length updates occurring at the quantum frequency,

$$\lambda_C, \qquad F_q,$$

which define the elementary spatial and temporal increments of the discrete Aether framework.

The present analysis is restricted to observables generated from

$$\chi_t, \qquad \tau_t, \qquad \delta\beta, \qquad \lambda_c, \qquad \xi_M, \qquad \mathrm{swep}, \qquad \mathrm{powr}.$$

The temporal sweep,

$$\mathrm{swep} = {\lambda_C}^2 F_q,$$

characterizes the transport of organized temporal domains, while the QMU power unit,

$$\mathrm{powr},$$

quantifies the rate of energetic transport associated with chronogeometric evolution.

The transport field is defined by

$$\mathbf{F} = -\nabla\chi_t + \gamma\nabla\tau_t,$$

where the first term represents transport driven by temporal-torque gradients and the second term represents transport associated with temporal twisting.

The filament handedness observable is

$$h_f = \hat{\mathbf{t}} \cdot (\nabla \times \mathbf{F}) \,.$$

Residual birefringence maps,

$$\delta\beta(\hat{\mathbf{n}}),$$

represent the projected observational manifestation of organized chronotorsional organization domains. Memory correlation lengths,

$$\xi_M(z),$$

characterize the persistence of organization as a function of cosmic time, while node connectivity statistics,

$$\langle k_n(z) \rangle,$$

quantify the degree of large-scale filamentary organization.

These quantities collectively define the complete observational inventory employed throughout the remainder of this paper.

4 Synthetic Sky Generation

The synthetic observational program begins with the temporal-torque simulations developed in Paper VII Thomson III [2026g]. Those simulations produced organized domains of chronotorsional curl-organization density,

$$\chi_t(\mathbf{x}),$$

and temporal twisting,

$$\tau_t(\mathbf{x}),$$

whose evolution generated coherent chronogeometric structures and persistent memory correlations.

The present work converts these three-dimensional chronogeometric fields into observable quantities by constructing synthetic residual birefringence maps,

$$\delta\beta(\hat{\mathbf{n}}),$$

on the celestial sphere. The underlying assumption is that organized chronotorsional organization domains induce small polarization rotations that preserve information regarding the integrated chronogeometric history encountered along each line of sight.

The residual birefringence field is generated through a line-of-sight projection of the organized chronotorsional organization fields,

$$\delta\beta(\hat{\mathbf{n}}) = A_\beta \int_0^{\chi_{\max}} \frac{\text{swep}}{\text{velc}} \left[\chi_t(\chi\hat{\mathbf{n}}) + \eta\, \tau_t(\chi\hat{\mathbf{n}}) + \zeta\, \hat{\mathbf{n}} \cdot \mathbf{F}(\chi\hat{\mathbf{n}}) \right] d\chi,$$

where

$$\chi$$

is the comoving distance and

$$A_\beta, \qquad \eta, \qquad \zeta$$

are dimensionless normalization coefficients.

The coefficients

$$A_\beta, \qquad \eta, \qquad \zeta$$

are introduced here solely to parameterize the projection operator in a manner suitable for observational implementation. They do not represent arbitrary degrees of freedom of the theory. In the full chronogeometric framework, these coefficients are expected to be constrained by QMU closure relations and by normalization to observational amplitudes. Their explicit derivation is deferred to future work.

The factor

$$\frac{\text{swep}}{\text{velc}}$$

weights the projection by the temporal sweep associated with discrete Compton-scale evolution.

The resulting birefringence maps are discretized using the HEALPix pixelization scheme [Górski et al., 2005] in order to permit direct comparison with observational products from cosmic microwave background polarization experiments.

The angular structure of the synthetic maps is quantified by the power spectra [Minami and Komatsu, 2020, Diego-Palazuelos et al., 2022]

$$C_\ell^{\beta\beta}, \qquad C_\ell^{E\beta}, \qquad C_\ell^{B\beta},$$

which measure, respectively, the auto-correlation of the birefringence field and its cross-correlations with the polarization modes of the microwave background.

For visualization and comparison purposes, the power is also represented as

$$D_\ell = \frac{\ell(\ell+1)}{2\pi} C_\ell^{\beta\beta}.$$

Within the chronogeometric interpretation, organized chronotorsional organization domains are expected to generate synthetic skies exhibiting several potentially observable characteristics.

First, long-lived temporal memory domains may generate excess power at low multipoles owing to their coherent angular extent.

Second, anisotropic organization may produce preferred directions or hemispherical asymmetries.

Third, the projection of filamentary structures may produce non-Gaussian morphologies and extended correlations between neighboring sky regions.

Finally, persistent temporal-torque organization may induce correlations between residual birefringence and independent tracers of large-scale structure.

These predictions are treated as hypotheses only. The purpose of constructing synthetic skies is not to establish detections but rather to generate reproducible observational templates that may be subjected to direct statistical comparison with observational data and null realizations.

5 Filament Catalog Comparisons

The filamentary organization predicted by the chronogeometric framework permits direct comparison with observational catalogs of large-scale structure.

Comparison templates are constructed from galaxy surveys that provide measurements of filament locations, orientations, and node connectivity [York et al., 2000, Dey et al., 2019, DESI Collaboration, 2016, European Space Agency, 2026]. Examples include products derived from the Sloan Digital Sky Survey (SDSS), the Dark Energy Spectroscopic Instrument (DESI), and future Euclid filament catalogs.

The principal observables are the filament orientation vector,

$$\hat{\mathbf{f}},$$

the handedness statistic,

$$h_f,$$

the node degree,

$$k_n,$$

and the memory correlation length,

$$\xi_M.$$

The memory correlation function is defined by

$$\xi_M(r) = \langle \chi_t(\mathbf{x}) \chi_t(\mathbf{x}+\mathbf{r}) \rangle \,,$$

which measures the persistence of temporal-torque organization between points separated by a distance

$$r.$$

The characteristic correlation length is extracted from the decay of this function and is denoted

$$\xi_M(z),$$

to emphasize its possible dependence upon redshift.

For direct comparison between simulations and observational catalogs, the memory correlation function is normalized according to

$$\xi_M^{\mathrm{QMU}}(r,z) = \frac{\langle \chi_t(\mathbf{x},z)\chi_t(\mathbf{x}+\mathbf{r},z)\rangle}{\langle \chi_t^2\rangle}.$$

The characteristic memory length,

$$\xi_M(z),$$

is defined as the separation satisfying

$$\xi_M^{\mathrm{QMU}} = e^{-1}.$$

This normalization permits direct comparison across redshifts, simulation realizations, and observational surveys while preserving the relative strength of chronogeometric organization.

Within the chronogeometric framework, coherent chronotorsional organization domains are expected to organize matter along preferred transport directions. Consequently, the predicted filamentary structures may exhibit non-random orientation statistics, coherent handedness distributions, and redshift-dependent memory lengths.

Node statistics provide an additional observable [Codis et al., 2018b]. The average node connectivity,

$$\langle k_n(z)\rangle,$$

quantifies the degree of filamentary organization and may provide an indirect measure of chronogeometric ordering.

The observational analysis therefore seeks to determine whether the measured orientation distributions, handedness statistics, and correlation lengths differ significantly from those expected from random realizations or conventional structure-formation scenarios.

No assumption is made regarding the existence of chronogeometric organization. Instead, filament catalogs are treated as independent observational laboratories within which the persistence of temporal memory may be tested statistically.

6 Cross-Correlation Statistics

The principal observational test of the chronogeometric hypothesis is the existence of statistically significant correlations between filamentary organization and residual birefringence.

The normalized handedness-birefringence correlation is defined by

$$C_{h\beta} = \frac{\langle h_f(\mathbf{x})\,\delta\beta(\hat{\mathbf{n}}(\mathbf{x}))\rangle}{\sigma_{h_f}\sigma_{\delta\beta}},$$

where

$$\sigma_{h_f}$$

and

$$\sigma_{\delta\beta}$$

are the standard deviations of the handedness and birefringence fields.

The filament-birefringence alignment statistic is

$$C_{f\beta} = \frac{\left\langle \hat{\mathbf{f}} \cdot \nabla\delta\beta \right\rangle}{\sigma_f \sigma_{\nabla\delta\beta}},$$

where

$$\sigma_f$$

and

$$\sigma_{\nabla\delta\beta}$$

represent the dispersions of the filament orientations and birefringence gradients.

If organized chronotorsional organization domains exist and persist over cosmological scales, then both statistics may exhibit measurable deviations from random expectations.

To quantify the statistical significance of these correlations, a memory detection statistic is introduced,

$$S_M = \frac{C_{h\beta}}{\sigma_{C_{h\beta}}},$$

where

$$\sigma_{C_{h\beta}}$$

denotes the uncertainty in the measured correlation.

The interpretation of this statistic is intentionally conservative.

Values satisfying

$$S_M \approx 0$$

indicate no evidence for persistent temporal memory.

Values satisfying

$$S_M > 3$$

may indicate evidence for organized chronotorsional organization domains.

Values satisfying

$$S_M > 5$$

constitute strong evidence that the observed correlations are inconsistent with random fluctuations.

An analogous significance measure may also be defined for the filament-alignment statistic,

$$S_A = \frac{C_{f\beta}}{\sigma_{C_{f\beta}}}.$$

The purpose of these statistics is not to demonstrate the correctness of the Aether interpretation. Rather, they provide reproducible measures of whether statistically significant memory signatures persist after observational uncertainties and null tests are taken into account.

6.1 Observational Implementation

Synthetic

$$\delta\beta(\hat{\mathbf{n}})$$

maps and

$$h_f$$

distributions generated from the temporal-torque evolution equations are cross-correlated with public filament catalogs and cosmic microwave background polarization products using the estimators defined above.

The resulting statistics are evaluated using Monte Carlo realizations, randomized skies, and conventional comparison suites.

A chronogeometric detection requires

$$S_M > 3$$

after all null tests and after subtraction of conventional baselines.

Strong evidence for persistent temporal memory requires

$$S_M > 5.$$

Equivalent thresholds may be defined for the alignment statistic,

$$S_A,$$

thereby providing independent measures of the significance of filament-birefringence organization.

7 Null Tests

A fundamental requirement of any observational claim is the demonstration that apparent correlations do not arise from chance alignments, survey geometry, instrumental effects, or statistical fluctuations.

For this reason, chronogeometric memory is intentionally destroyed through a sequence of null experiments.

The first null test employs phase randomization of the birefringence field,

$$\delta\beta \to \delta\beta_{\mathrm{rand}},$$

which preserves the power spectrum while eliminating coherent spatial organization.

The second test employs handedness scrambling,

$$h_f \to \pm h_f,$$

which destroys coherent chirality while preserving the underlying filament network.

The third test applies random filament reorientations,

$$\hat{\mathbf{f}} \to R(\theta,\phi)\hat{\mathbf{f}},$$

where

$$R(\theta,\phi)$$

represents an arbitrary rotational operator.

The fourth test rotates the sky itself,

$$\hat{\mathbf{n}} \to R\hat{\mathbf{n}},$$

thereby removing preferred alignments between sky features and filament orientations.

Finally, instrumental and reconstruction uncertainties are represented through noise realizations,

$$\delta\beta \to \delta\beta + N,$$

where

$$N$$

denotes a statistically generated noise field.

After each operation, the correlation statistics

$$C_{f\beta} \qquad \text{and} \qquad C_{h\beta}$$

are recomputed.

If the chronogeometric observables arise solely from random fluctuations, their statistical significance should remain unchanged under these transformations.

Conversely, if the observed correlations originate from persistent temporal-torque organization, then the destruction of memory should produce statistically significant reductions in the measured correlations.

The null tests therefore constitute one of the most important components of the observational program, since they determine whether apparent memory signatures represent genuine organization or merely statistical artifacts.

8 Conventional Model Comparisons

The observational signatures proposed in this paper acquire scientific value only if they remain distinguishable from the signatures generated by conventional theories of structure formation. Consequently, every chronogeometric observable is compared directly against established models that do not invoke temporal-torque organization.

The first comparison class consists of gravitational density-field models in which matter clustering is governed by the gravitational potential,

$$\nabla^2 \Phi_G = 4\pi G \rho.$$

Such models naturally produce filaments and nodes through gravitational collapse and anisotropic matter accretion [Zel'dovich, 1970, Forero-Romero et al., 2009, Sousbie, 2011, Sousbie et al., 2011]. The resulting filament orientations and connectivity statistics therefore provide an essential baseline against which chronogeometric predictions must be measured.

The second comparison class consists of tidal-torque models in which angular momentum is generated by interactions between the local inertia tensor and the surrounding tidal field. The angular momentum vector may be expressed schematically as

$$L_i = \epsilon_{ijk} I_{jl} T_{lk},$$

where

$$I_{jl}$$

is the inertia tensor and

$$T_{lk}$$

is the tidal tensor.

Tidal-torque theory predicts preferred orientation statistics and spin correlations that may superficially resemble temporal-memory signatures [Peebles, 1969, White, 1984, Codis et al., 2018a, Wang et al., 2021]. The present analysis therefore explicitly tests whether the handedness statistics predicted by the chronogeometric framework reduce to tidal-torque correlations.

The third comparison class consists of reaction-diffusion systems governed by equations of the form

$$\frac{\partial u}{\partial t} = D\nabla^2 u + R(u),$$

where

$$D$$

is an effective diffusion coefficient and

$$R(u)$$

represents nonlinear interactions.

Reaction-diffusion systems naturally generate filaments, domains, and coherent patterns and therefore provide an important null hypothesis for the organization of large-scale structure [Allen and Cahn, 1979, Bray, 1994].

The fourth comparison class consists of generic phase-ordering systems governed by equations such as

$$\frac{\partial \psi}{\partial t} = D\nabla^2 \psi - V'(\psi),$$

where

$$\psi$$

denotes an order parameter and

$$V(\psi)$$

represents an effective potential.

Phase-ordering dynamics produce domain formation and coarsening phenomena that may generate long-range correlations and apparent memory effects [Bray, 1994].

The central question of this section is therefore straightforward:

Do the observables generated from

$$\chi_t \qquad \text{and} \qquad \tau_t$$

reduce entirely to statistics already predicted by conventional theories, or do they retain distinct signatures of persistent chronogeometric organization?

The answer determines whether temporal-torque memory represents a genuinely new observational hypothesis or merely a reformulation of known structure-formation mechanisms.

In practice, all synthetic observables generated from the chronogeometric simulations are subjected to the same statistical estimators employed for the conventional comparison suites. Residual birefringence maps, handedness distributions, coherence lengths, and node statistics are analyzed identically so that any differences arise from the underlying organization of the models rather than from differences in methodology.

A distinct chronogeometric signature requires that multiple observables simultaneously exhibit statistically significant departures from the predictions of all conventional comparison classes. No individual observable is regarded as sufficient evidence in isolation.

9 Statistical Inference

The observational program developed in this paper is fundamentally statistical in nature. Every predicted observable is therefore quantified through reproducible significance measures and goodness-of-fit estimators.

The primary goodness-of-fit statistic is

$$\chi^2 = \sum_i \frac{(O_i - M_i)^2}{\sigma_i^2},$$

where

$$O_i$$

denotes the observational measurement,

$$M_i$$

denotes the corresponding model prediction, and

$$\sigma_i$$

represents the observational uncertainty.

Separate goodness-of-fit statistics are computed for the residual birefringence spectra, filament orientation statistics, handedness distributions, node connectivity measurements, and memory correlation lengths.

Direct model comparisons are quantified through

$$\Delta\chi^2 = \chi^2_{\mathrm{QMU}} - \chi^2_{\Lambda\mathrm{CDM}}.$$

Negative values of

$$\Delta\chi^2$$

indicate that the chronogeometric model provides a better description of the observational data than the reference cosmological model, whereas positive values indicate the opposite.

Because more complicated models can artificially improve goodness of fit, information criteria are also employed [Akaike, 1974, Schwarz, 1978]. The Akaike Information Criterion is defined by

$$\mathrm{AIC} = 2k + \chi^2,$$

where

$$k$$

is the number of fitted parameters.

Similarly, the Bayesian Information Criterion is

$$\mathrm{BIC} = k \ln N + \chi^2,$$

where

$$N$$

denotes the number of independent measurements.

These information criteria penalize unnecessary model complexity and therefore discourage overfitting.

The memory detection statistic,

$$S_M = \frac{C_{h\beta}}{\sigma_{C_{h\beta}}},$$

provides an independent measure of the statistical significance of persistent temporal-torque organization.

An analogous statistic,

$$S_A = \frac{C_{f\beta}}{\sigma_{C_{f\beta}}},$$

quantifies the significance of filament-birefringence alignment.

A complementary measure of persistent chronogeometric organization is provided by the memory excess statistic,

$$E_M = \frac{\xi_M^{\mathrm{QMU}} - \xi_M^{\mathrm{null}}}{\sigma_\xi},$$

where

$$\xi_M^{\mathrm{null}}$$

is the memory correlation length obtained from randomized realizations and

$$\sigma_\xi$$

denotes the uncertainty in the correlation-length estimator.

The interpretation of this statistic parallels that of the correlation significances.

Values satisfying

$$E_M \approx 0$$

indicate no measurable excess memory beyond that expected from random realizations.

Values satisfying

$$E_M > 3$$

indicate evidence for persistent chronogeometric organization.

Values satisfying

$$E_M > 5$$

constitute strong evidence that the observed coherence lengths exceed those generated by statistical fluctuations or null models.

Monte Carlo realizations are used to estimate the distributions of all test statistics under the null hypothesis. The resulting significance levels therefore incorporate the effects of finite survey volumes, noise realizations, reconstruction uncertainties, and accidental alignments.

No statistical estimator is interpreted in isolation. Instead, the observational viability of the chronogeometric hypothesis is determined by the collective behavior of the full ensemble of observables and their associated significance measures.

10 Falsification Criteria

The purpose of the present paper is not to establish the correctness of the Aether Physics Model. Rather, the purpose is to determine whether the observational consequences of organized chrono-

Table 1: Principal chronogeometric observables and their falsifiable predictions.

Observable	QMU Origin	Predicted Signature
$\delta\beta(\hat{\mathbf{n}})$	χ_t, τ_t	Large-scale coherent anisotropy
h_f	$\nabla \times \mathbf{F}$	Non-random handedness distribution
$\xi_M(z)$	Temporal memory persistence	Redshift-dependent coherence length
$C_{h\beta}$	Temporal-memory projection	Nonzero handedness-birefringence correlation
$C_{f\beta}$	Transport organization	Filament-birefringence alignment

torsional organization domains survive direct empirical scrutiny. The observational status of the chronogeometric hypothesis is therefore determined jointly by the statistics

$$S_M, \qquad S_A, \qquad E_M,$$

which respectively measure handedness memory, filament-birefringence alignment, and excess persistence of temporal organization.

For this reason, explicit conditions are specified under which the chronogeometric interpretation is not observationally supported.

The first condition is the absence of measurable memory correlations,

$$S_M \approx 0.$$

Under this circumstance, residual birefringence fields and filament handedness exhibit no statistically significant relationship.

The second condition is the absence of measurable alignment correlations,

$$S_A \approx 0.$$

This result indicates that filament orientations are statistically independent of birefringence gradients.

The third condition is the absence of persistent memory lengths,

$$\xi_M(z),$$

or the demonstration that any measured coherence lengths are entirely consistent with random realizations.

The fourth condition is that the handedness distributions become statistically indistinguishable from those produced by random fields or conventional structure-formation models.

The fifth condition is that all observed signatures can be reproduced simultaneously by gravitational density-field models, tidal-torque theory, reaction-diffusion systems, or generic phase-ordering dynamics.

If these conditions are satisfied, then the proposed five-dimensional chronogeometric interpretation is not observationally supported.

Conversely, the chronogeometric hypothesis remains observationally viable if the following conditions are simultaneously satisfied:

1. statistically significant values of
$$S_M$$
persist after all null tests;
2. statistically significant values of
$$S_A$$
remain after phase randomization and sky rotations;
3. memory lengths
$$\xi_M(z)$$
exhibit coherent evolution with redshift;
4. filament handedness distributions differ significantly from random expectations;
5. no conventional comparison model reproduces the full ensemble of observables simultaneously.

The requirement that multiple independent observables survive direct confrontation with the data intentionally establishes a high evidentiary threshold.

Accordingly, the five-dimensional Aether framework remains a falsifiable scientific hypothesis whose observational status depends entirely upon whether persistent chronogeometric memory signatures survive empirical comparison with the sky.

11 Future Observational Programs

The observational program developed in this paper is intended to provide a reproducible framework for testing chronogeometric memory using current and forthcoming cosmological surveys. The methodology deliberately separates theoretical assumptions from observational procedures so that every predicted signature may be subjected to independent verification or falsification.

Future measurements of cosmic microwave background polarization are expected to improve sensitivity to residual birefringence fields and large-scale angular correlations [LiteBIRD Collaboration, 2023, Collaboration, 2021, Abazajian et al., 2016, JAXA Institute of Space and Astronautical Science, 2026]. In particular, upcoming polarization surveys will provide increasingly precise measurements of

$$C_\ell^{\beta\beta}, \qquad C_\ell^{E\beta}, \qquad C_\ell^{B\beta},$$

thereby permitting direct tests of the synthetic birefringence templates generated from temporal-torque simulations.

Likewise, next-generation large-scale structure surveys will substantially improve measurements of filamentary organization, node connectivity, and orientation statistics [DESI Collaboration, 2016, European Space Agency, 2026]. Expanded spectroscopic and photometric galaxy catalogs will permit more accurate determinations of

$$h_f, \qquad \langle k_n(z)\rangle, \qquad \xi_M(z),$$

and their possible redshift evolution.

Particularly promising are joint analyses combining polarization measurements and large-scale structure catalogs. Such analyses permit direct evaluation of the cross-correlation statistics

$$C_{f\beta} = \mathrm{corr}\left(\hat{\mathbf{f}}, \nabla\delta\beta\right),$$

and

$$C_{h\beta} = \mathrm{corr}\left(h_f, \delta\beta\right).$$

The memory detection statistic,

$$S_M = \frac{C_{h\beta}}{\sigma_{C_{h\beta}}},$$

may therefore be evaluated using progressively larger and more precise observational datasets.

Future surveys also permit increasingly stringent null tests. Phase randomization, sky rotations, handedness scrambling, and noise realizations may be performed on larger observational samples and with improved control of systematic uncertainties. Consequently, apparent correlations that arise from survey geometry, reconstruction artifacts, or statistical fluctuations should become increasingly distinguishable from genuine cosmological organization.

The observational program proposed here therefore makes several concrete predictions that may be tested directly:

1. Residual birefringence maps may exhibit coherent low-multipole structures correlated with filamentary organization.
2. Filament handedness distributions may exhibit departures from purely random expectations.
3. Memory correlation lengths,
$$\xi_M(z),$$
may evolve systematically with redshift.
4. Filament orientations and birefringence gradients may exhibit statistically significant alignment correlations.
5. Multiple independent observables may simultaneously exhibit memory signatures that survive null tests and cannot be reproduced by conventional comparison models.

Equally important, future observations may falsify the entire chronogeometric interpretation. If increasingly precise measurements demonstrate that

$$S_M \approx 0, \qquad S_A \approx 0,$$

that coherence lengths remain consistent with random realizations, and that all observed statistics are fully reproducible by conventional models of structure formation, then the proposed five-dimensional chronogeometric interpretation is not observationally supported.

The observational framework presented here therefore represents not a claim of detection, but rather a reproducible program for determining whether organized chronotorsional organization domains leave measurable imprints in cosmic birefringence and filamentary large-scale structure. The ultimate status of the discrete five-dimensional Aether framework consequently rests upon direct comparison with the sky itself.

The observational significance of the present program extends beyond the detection of any particular signal. If multiple independent observables derived from the same chronogeometric quantities survive null tests and remain statistically distinct from conventional baselines, then the quantities

$$\chi_t, \qquad \tau_t, \qquad \mathbf{F}, \qquad \xi_M,$$

acquire operational meaning as measurable descriptors of cosmological organization. In that circumstance, chronogeometry ceases to be merely a formal construction and becomes an empirically defined dynamical geometry whose properties are inferred directly from reproducible observations.

12 Conclusions

The preceding papers of this series established a discrete five-dimensional chronogeometric framework, developed quantitative temporal-torque observables in Quantum Measurement Units, derived filamentary organization laws, formulated evolution equations, and generated synthetic numerical predictions.

The present work has completed the transition from numerical prediction to observational confrontation.

Synthetic residual birefringence maps, filament orientation statistics, handedness distributions, node connectivity measurements, and memory correlation lengths have been formulated as reproducible observational products derived directly from previously established QMU quantities.

Equally important, these observables have been subjected to explicit null tests and direct comparisons with conventional theories of structure formation.

The purpose of this paper has therefore been intentionally conservative. No observational detections have been assumed. No claim has been made that organized chronotorsional organization domains exist in nature. Every prediction remains provisional until confronted by observational data.

Instead, the present work establishes a reproducible observational pipeline by which the temporal-torque memory hypothesis may be falsified.

If residual birefringence fields, filament handedness statistics, node connectivity measurements, and redshift-dependent coherence lengths exhibit no statistically significant memory correlations beyond those predicted by conventional models, then the proposed chronogeometric interpretation is not observationally supported.

Conversely, if multiple independent observables survive null tests and retain statistically significant correlations that cannot be reproduced by conventional theories, then the Aether Physics Model acquires a distinct empirical signature whose origin requires further investigation.

The present paper therefore concludes with one question and one question only:

Can the discrete five-dimensional Aether unit produce observable memory signatures

that survive direct confrontation with the sky?

Acknowledgments

The Quantum AetherDynamics Institute (QADI) is a private 501(c)(3) research institute developing the Aether Physics Model (APM) and Quantum Measurement Units (QMU) Thomson III [2025]. Publications and data are archived with DOIs in the AetherPhysics Zenodo community: zenodo.org/communities/aetherphysics.

References

K. N. Abazajian et al. CMB-S4 science book, first edition, 2016.

H. Akaike. A new look at the statistical model identification. *IEEE Transactions on Automatic Control*, 19(6):716–723, 1974. doi: 10.1109/TAC.1974.1100705.

S. M. Allen and J. W. Cahn. A microscopic theory for antiphase boundary motion and its application to antiphase domain coarsening. *Acta Metallurgica*, 27(6):1085–1095, 1979. doi: 10.1016/0001-6160(79)90196-2.

A. J. Bray. Theory of phase-ordering kinetics. *Advances in Physics*, 43(3):357–459, 1994. doi: 10.1080/00018739400101505.

S. Codis, A. Jindal, N. E. Chisari, D. Vibert, Y. Dubois, C. Pichon, and J. Devriendt. Galaxy orientation with the cosmic web across cosmic time. *Monthly Notices of the Royal Astronomical Society*, 481(4):4753–4774, 2018a. doi: 10.1093/mnras/sty2567.

S. Codis, C. Pichon, and D. Pogosyan. Connectivity of the cosmic web. *Monthly Notices of the Royal Astronomical Society*, 479(1):973–993, 2018b. doi: 10.1093/mnras/sty1515.

LiteBIRD Collaboration. LiteBIRD: JAXA's New Strategic L-Class Mission for All-Sky Surveys of Cosmic Microwave Background Polarization. *arXiv preprint arXiv:2101.12449*, 2021.

DESI Collaboration. The DESI experiment part i: Science, targeting, and survey design, 2016.

A. Dey et al. Overview of the DESI legacy imaging surveys. *The Astronomical Journal*, 157(5):168, 2019. doi: 10.3847/1538-3881/ab089d.

P. Diego-Palazuelos, J. R. Eskilt, Y. Minami, M. Tristram, R. M. Sullivan, A. J. Banday, R. B. Barreiro, H. K. Eriksen, K. M. G'orski, R. Keskitalo, E. Komatsu, E. Mart'inez-Gonz'alez, D. Scott, P. Vielva, and I. K. Wehus. Cosmic birefringence from planck public release 4. *Physical Review Letters*, 128:091302, 2022. doi: 10.1103/PhysRevLett.128.091302.

European Space Agency. Euclid Overview, 2026. URL `https://www.esa.int/Science_Exploration/Space_Science/Euclid_overview`.

J. E. Forero-Romero, Y. Hoffman, S. Gottl"ober, A. Klypin, and G. Yepes. A dynamical classification of the cosmic web. *Monthly Notices of the Royal Astronomical Society*, 396(3):1815–1824, 2009. doi: 10.1111/j.1365-2966.2009.14885.x.

K. M. Górski, E. Hivon, A. J. Banday, B. D. Wandelt, F. K. Hansen, M. Reinecke, and M. Bartelmann. HEALPix: A framework for high-resolution discretization and fast analysis of data distributed on the sphere. *The Astrophysical Journal*, 622(2):759–771, 2005. doi: 10.1086/427976.

JAXA Institute of Space and Astronautical Science. LiteBIRD: Lite Satellite for the Studies of B-mode Polarization and Inflation from Cosmic Background Radiation Detection, 2026. URL https://www.isas.jaxa.jp/en/missions/spacecraft/future/litebird.html.

LiteBIRD Collaboration. Probing cosmic inflation with the litebird cosmic microwave background polarization survey. *Progress of Theoretical and Experimental Physics*, 2023(4):042F01, 2023. doi: 10.1093/ptep/ptac150.

Y. Minami and E. Komatsu. New extraction of the cosmic birefringence from the planck 2018 polarization data. *Physical Review Letters*, 125:221301, 2020. doi: 10.1103/PhysRevLett.125.221301.

P. J. E. Peebles. Origin of the angular momentum of galaxies. *The Astrophysical Journal*, 155:393, 1969. doi: 10.1086/149876.

G. Schwarz. Estimating the dimension of a model. *The Annals of Statistics*, 6(2):461–464, 1978. doi: 10.1214/aos/1176344136.

T. Sousbie. The persistent cosmic web and its filamentary structure – i. theory and implementation. *Monthly Notices of the Royal Astronomical Society*, 414(1):350–383, 2011. doi: 10.1111/j.1365-2966.2011.18394.x.

T. Sousbie, C. Pichon, and H. Kawahara. The persistent cosmic web and its filamentary structure – ii. illustrations. *Monthly Notices of the Royal Astronomical Society*, 414(1):384–403, 2011. doi: 10.1111/j.1365-2966.2011.18395.x.

David W. Thomson III. Quantum aetherdynamics institute (qadi): Community doi overview and citation guide. Zenodo, 2025. URL https://doi.org/10.5281/zenodo.17479314.

David W. Thomson III. Aether tomography: Residual cosmic birefringence as a probe of organized five-dimensional chronogeometric structure, June 2026a. URL https://doi.org/10.5281/zenodo.20754696.

David W. Thomson III. Temporal-torque evolution and the dynamics of filamentary chronogeometry: A predictive theory of chronogeometric growth, domain evolution, and cosmic-web memory, jun 2026b. URL https://doi.org/10.5281/zenodo.20798552.

David W. Thomson III. Filamentary chronogeometry and large-scale aether organization: A predictive theory of temporal-torque corridors and cosmic filament structure, jun 2026c. URL https://doi.org/10.5281/zenodo.20788913.

David W. Thomson III. Numerical reconstruction of organized temporal-torque domains and simulated residual cosmic birefringence maps, June 2026d. URL https://doi.org/10.5281/zenodo.20779504.

David W. Thomson III. Quantitative definition of temporal torque density and chronotorsional holonomy: A qmu derivation of organized five-dimensional chronogeometric structure, June 2026e. URL https://doi.org/10.5281/zenodo.20778298.

David W. Thomson III. Temporal torque memory and galactic-scale aether organization: A predictive framework for cosmic birefringence, June 2026f. URL https://doi.org/10.5281/zenodo.20753446.

David W. Thomson III. Qmu-constrained simulation of temporal-torque evolution: Numerical chronogeometric domains, filament memory, and synthetic birefringence observables, June 2026g. URL https://zenodo.org/records/20806198.

P. Wang, N. I. Libeskind, E. Tempel, X. Kang, and Q. Guo. Possible observational evidence for cosmic filament spin. *Nature Astronomy*, 5:839–845, 2021. doi: 10.1038/s41550-021-01380-6.

S. D. M. White. Angular momentum growth in protogalaxies. *The Astrophysical Journal*, 286:38–41, 1984. doi: 10.1086/162573.

D. G. York et al. The sloan digital sky survey: Technical summary. *The Astronomical Journal*, 120 (3):1579–1587, 2000. doi: 10.1086/301513.

Ya. B. Zel'dovich. Gravitational instability: An approximate theory for large density perturbations. *Astronomy and Astrophysics*, 5:84–89, 1970.